Nat. Hazards Earth Syst. Sci., 15, 1407–1423, 2015
www.nat-hazards-earth-syst-sci.net/15/1407/2015/
doi:10.5194/nhess-15-1407-2015

Natural Hazards and Earth System Sciences
Open Access

Development of a Global Fire Weather Database

R. D. Field[1,2], A. C. Spessa[3,4], N. A. Aziz[5], A. Camia[6], A. Cantin[7], R. Carr[8], W. J. de Groot[7], A. J. Dowdy[9], M. D. Flannigan[10,11], K. Manomaiphiboon[12], F. Pappenberger[13,14,15], V. Tanpipat[12], and X. Wang[10]

[1]Department of Applied Physics and Applied Mathematics, Columbia University, New York, NY, USA
[2]NASA Goddard Institute for Space Studies, New York, NY, USA
[3]Department Environment, Earth & Ecosystems, The Open University, Milton Keynes, UK
[4]Department Atmospheric Chemistry, Max Planck Institute for Chemistry, Mainz, Germany
[5]Malaysian Meteorological Department, Petaling Jaya, Malaysia
[6]Joint Research Centre, European Commission, Ispra, Italy
[7]Natural Resources Canada, Canadian Forest Service, Sault Ste. Marie, ON, Canada
[8]Natural Resources Canada, Canadian Forest Service, Edmonton, AB, Canada
[9]The Centre for Australian Weather and Climate Research, Australian Bureau of Meteorology, Victoria, Australia
[10]Department of Renewable Resources, University of Alberta, Edmonton, AB, Canada
[11]Western Partnership on Wildland Fire Science, Edmonton, AB, Canada
[12]The Joint Graduate School of Energy and Environment, King Mongkut's University of Technology Thonburi, Bangkok, Thailand
[13]European Centre for Medium-Range Weather Forecasts, Reading, UK
[14]College of Hydrology and Water Resources, Hohai University, Nanjing, China
[15]School of Geographical Sciences, Bristol University, Bristol, UK

Correspondence to: R. D. Field (robert.field@columbia.edu)

Received: 19 August 2014 – Published in Nat. Hazards Earth Syst. Sci. Discuss.: 17 October 2014
Revised: 16 May 2015 – Accepted: 18 May 2015 – Published: 30 June 2015

Abstract. The Canadian Forest Fire Weather Index (FWI) System is the mostly widely used fire danger rating system in the world. We have developed a global database of daily FWI System calculations, beginning in 1980, called the Global Fire WEather Database (GFWED) gridded to a spatial resolution of 0.5° latitude by 2/3° longitude. Input weather data were obtained from the NASA Modern Era Retrospective-Analysis for Research and Applications (MERRA), and two different estimates of daily precipitation from rain gauges over land. FWI System Drought Code calculations from the gridded data sets were compared to calculations from individual weather station data for a representative set of 48 stations in North, Central and South America, Europe, Russia, Southeast Asia and Australia. Agreement between gridded calculations and the station-based calculations tended to be most different at low latitudes for strictly MERRA-based calculations. Strong biases could be seen in either direction: MERRA DC over the Mato Grosso in Brazil reached unrealistically high values exceeding DC = 1500 during the dry season but was too low over Southeast Asia during the dry season. These biases are consistent with those previously identified in MERRA's precipitation, and they reinforce the need to consider alternative sources of precipitation data. GFWED can be used for analyzing historical relationships between fire weather and fire activity at continental and global scales, in identifying large-scale atmosphere–ocean controls on fire weather, and calibration of FWI-based fire prediction models.

1 Introduction

Fire danger rating systems are used to identify conditions under which vegetation fires can start and spread (Merrill and Alexander, 1987). This is done by modeling the moisture content of different classes of fuels in response to changing weather conditions, and potential fire behavior if a fire were to start. The Canadian Forest Fire Weather Index (FWI, see

Table 1. Acronyms used in the paper.

Acronym	Definition
ASEAN	Association of Southeast Asian Nations
BoM	Australian Bureau of Meteorology
BUI	Buildup Index
CFS	Canadian Forest Service
CPC	Climate Prediction Center precipitation (Chen et al., 2008)
CRU	Climate Research Unit
CWFIS	Canadian Wildland Fire Information System
DC	Drought Code
DMC	Duff Moisture Code
DSR	Daily Severity Rating
EnvCan	Environment Canada
FFMC	Fine Fuel Moisture Code
FWI	Fire Weather Index
GFWED	Global Fire Weather Database
GLFC	Great Lakes Forestry Centre
GPM	Global Precipitation Measurement
GTS	Global Telecommunications System
ISI	Initial Spread Index
ITCZ	Intertropical Convergence Zone
KLIA	Kuala Lumpur International Airport
LT	Local time
MERRA	Modern Era Retrospective-Analysis for Research and Applications (Rienecker et al., 2011)
MMD	Malaysian Meteorological Department
MODIS	Moderate Resolution Imaging Spectroradiometer
NCAR	National Center for Atmospheric Research
NCDC ISD	National Climatic Data Center Integrated Surface Database
NCEP	National Centers for Environmental Prediction
NOAA	National Oceanic and Atmospheric Admininstration
NoFC	Northern Forestry Centre
NWP	Numerical Weather Prediction
QuickScat	Quick Scatterometer
SHEFF	Sheffield precipitation (Sheffield et al., 2006)
SMAP	Soil Moisture Active Passive
SMOS	Soil Moisture Ocean Salinity
SSM/I	Special Sensor Microwave Imager
TMD	Thailand Meteorological Department
TRMM	Tropical Rainfall Measuring Mission
UEA	University of East Anglia
WMO	World Meteorological Organization

list of acronyms in Table 1) System (Van Wagner, 1987) is the most widely used fire danger rating system in the world (de Groot and Flannigan, 2014). It has operated in its current form in Canada since 1970, and certain components have been adapted for operational use in New Zealand, Fiji, parts of the United States, Mexico, Argentina, Spain, Portugal, Indonesia, Malaysia, and Finland (Taylor and Alexander, 2006) and regionally across Europe (Camia and Amatulli, 2009). It has been used for estimating future activity in boreal regions (de Groot et al., 2013) and globally (Flannigan et al., 2013) under different climate change scenarios. Because of its use in such a broad range of fire environments, it is central to the ongoing development of real-time global fire danger rating systems (de Groot et al., 2006).

Use of the FWI System either operationally or for research purposes begins with experimental fires and laboratory experiments when possible, expert consultation, and historical analyses of FWI variability and relationships to past fire activity. Historical analyses are possible only after hourly measurements of surface temperature, humidity, wind speed and precipitation are compiled for as many years as available. Typically, these data are from surface weather station networks, and require significant effort in constructing a gap-free record, which is critical (Lawson and Armitage, 2008). FWI System maps are usually calculated from geostatistically interpolated weather fields from the individual stations (Lee et al., 2002).

Recent work has been done to calculate FWI System values from meteorological reanalyses over Portugal and Spain (Bedia et al., 2012), the whole of Europe (Camia and Amatulli, 2010) the Great Lakes region of the US (Horel et al., 2014) and Siberia (Chu and Guo, 2014) and globally for use as a baseline against which fire danger in a changing climate can be assessed (Flannigan et al., 2013). Reanalysis products have their own biases, but remain a critical research tool because of their overall utility (Rienecker et al., 2011). For the purposes of historical FWI System calculations, they have the advantages over raw weather station data of providing spatially and temporally continuous records based on estimates of weather input fields using the internal, physical consistency of a numerical weather prediction model and modern data assimilation techniques. We argue that reanalysis estimates provide the only practical means possible of calculating FWI values consistently at continental scales.

This paper describes our development of a global FWI data set for the period 1980–2012 gridded to a resolution of 0.5° latitude by 2/3° longitude based on the National Aeronautics and Space Administration (NASA) Modern Era Retrospective-Analysis for Research and Applications (MERRA) (Rienecker et al., 2011). Because precipitation in reanalyses tends to be less well-constrained by observations, we also use two global, gridded precipitation data sets. Our goals were to

1. provide easily accessible historical FWI System data for new regions of interest,

2. provide a consistent and homogenized product for continental and global-scale FWI analyses and

3. provide a product that can be easily updated and expanded over time.

This paper is organized as follows. In Sect. 2, we describe the FWI System components, their input data requirements and procedures for starting and stopping the calculations in cold regions. In Sect. 3, we describe the meteorological fields used to construct the gridded database and the weather station data against which we compare the gridded calculations. In Sect. 4, we compare the gridded Drought Code calculations to those from 48 individual weather stations across a representative set of locations, along with a brief description of global patterns in the Fire Weather Index. In Sect. 5, we summarize the results and suggest options for future GFWED development.

2 Description of the FWI System

The FWI System is composed of three moisture codes and three fire behavior indices (Van Wagner, 1987). The moisture codes track the moisture content of litter and forest floor moisture content rather, in general, than live fuel moisture. For all codes, increasing values reflect decreasing moisture content, and "extreme" thresholds are drawn from the Canadian Wildland Fire Information System (CWFIS, http://cwfis.nrcan.gc.ca), but these will be different in other regions. The Fine Fuel Moisture Code (FFMC) is designed to capture changes in the moisture content of fine fuels and leaf litter on the forest floor where fires can most easily start. The FFMC ranges from 0 to 99, with values greater than 91 classified as extreme. The Duff Moisture Code (DMC) captures the moisture content of loosely compacted forest floor organic matter and relates to the likelihood of lightning ignition. The DMC has no upper limit, but values greater than 60 are considered extreme. The Drought Code (DC) captures the moisture content of deep, compacted organic soils and heavy surface fuels. The DC also has no upper limit, but values greater than 425 are considered extreme. The three moisture codes are calculated on a daily basis using the previous day's moisture codes and the current day's weather. The three fire behavior indices reflect the behavior of a fire if it were to start. The Initial Spread Index (ISI) is driven by wind speed and FFMC and represents the ability of a fire to spread immediately after ignition, with values greater than 15 considered extreme. The Buildup Index (BUI) is driven by the DMC and DC and represents the total fuel available to a fire, with values greater than 90 considered extreme. The Fire Weather Index (FWI) combines the ISI and BUI to provide an overall rating of fireline intensity in a reference fuel type and level terrain, with values greater than 30 considered extreme. Additionally, the Daily Severity Rating (DSR) is scaled from the FWI to provide categorical difficulty of control measures. The fire behavior indices reflect surface weather conditions and do not reflect dryness or stability aloft which can also strongly influence fire behavior (Haines, 1988). Dowdy et al. (2009) provide an accessible description of the underlying equations. Taylor and Alexander (2006) summarize the history behind the FWI System and how different fire management agencies have adopted different components for specific fire management needs.

FWI System calculations require measurements of 12:00 local time (LT) instantaneous temperature at 2 m, relative humidity at 2 m and sustained wind speed at 10 m, and precipitation totaled over the previous 24 h (van Wagner, 1987). Measurements are taken in a clearing but the FWI System was designed such that the indices are representative of the conditions within a forest stand (Lawson and Armitage, 2008). Because each day's calculation requires the previous day's moisture codes, weather records must be continuous and any missing data must be estimated (Lawson and Armitage, 2008). Too much missing weather data, particularly precipitation, can lead to errors that accumulate over time.

In cold regions, the calculations begin with the arrival of spring and are stopped with the onset of winter (Lawson and Armitage, 2008). Ideally, the spring startup moisture code values reflect whether or not winter was dry, however this is defined. We based our startup approach on that of the Canadian Wildland Fire Information System (CWFIS), described at: http://cwfis.cfs.nrcan.gc.ca/background/dsm/fwi. First, snow conditions are examined for the possibility of startup after a winter with substantial snow cover, defined as having a mean snow depth of 10 cm or greater and snow present for a minimum of 75 % of days during the 2 months prior to startup. This requirement was modified from the CWFIS approach of considering snow days in January and February to allow for seasonality in regions other than Canada. In this case, startup occurs when the station has been snow-free for 3 consecutive days, and moisture code values representing wet, saturated conditions (DMC = 6, DC = 15) are used. For locations without significant snow cover, startup occurs when the mean daily temperature is 6 °C or greater for 3 consecutive days. The DMC is set to 2 times the number of days since precipitation and the DC is set to 5 times the number of days since precipitation. The FFMC is set to 85, regardless of whether significant winter snow cover was present because of its short memory, with a timelag of 3 days required to lose 2/3 of the free moisture content in light, fine fuels for a standard drying day in Canada, defined as having noon temperature of 21.1 °C and 45 % RH. The timelag for DMC fuels is 14 days (rather than the 12 days stated in Van Wagner (1987), S. Taylor, personal communication, 2015), and 51 days for DC, reflecting longer equilibration times. The calculations are stopped with either the arrival of snow or a mean temperature below 6 °C for three consecutive days.

This approach was chosen to capture the effect of winters with below-normal precipitation, but to avoid fuel and site-specific parameters described in the approach of Lawson and Armitage (2008), which required too much local expert knowledge for our global scope. We also masked out fire-free regions for which the FWI System calculations are not meaningful. Cold regions were excluded based on the requirement that mean annual temperature be greater than −10 °C. Desert regions were excluded based on the requirement that mean annual precipitation be greater than 0.25 mm day^{-1}. Cells where these criteria were not met were excluded for all years. Based on the temperature criteria, parts of the Canadian and Russian high Arctic were excluded. Based on the precipitation criteria, the Sahara, Gobi and much of the Arabian Peninsula were excluded. Mean annual temperature and rainfall fields are provided as part of the data distribution.

3 Weather data

In this section we describe the meteorological fields used for the gridded FWI calculations and the individual stations from regional agencies and data repositories against which the gridded calculations were compared. All data are available as part of the distribution, as is contact information for individual agency sources.

3.1 Gridded fields

The starting point for our calculations was the NASA Modern Era Retrospective-Analysis for Research and Applications (MERRA, Rienecker et al., 2011). MERRA is NASA's state-of-the-art reanalysis product which uses the GEOS 5 atmospheric general circulation model run at 1/2° latitude × 2/3° longitude horizontal resolution and with 72 vertical levels. Sea surface temperature and sea ice boundary conditions are prescribed from Reynolds et al. (2002). Observational constraints from a wide variety of in situ and remotely sensed sources are used. Pressure, temperature, humidity and wind observations are obtained from surface weather stations, upper air stations, aircraft reports and dropsondes, ship and buoy observations, as well as weather satellites and research instruments such as the Moderate Resolution Imaging Spectroradiometer (MODIS) and Quick Scatterometer (QuikSCAT). Raw radiance data are assimilated directly from microwave and infrared sounders with different observational periods, using embedded forward radiative transfer models to estimate instrument-equivalent fields. Precipitation is constrained most directly from Special Sensor Microwave Imager (SSM/I) radiances and Tropical Rainfall Measuring Mission (TRMM) rain rate estimates when available, but not by surface gauges. Further details are provided by Rienecker et al. (2011) and references therein.

Among FWI input variables, the MERRA precipitation estimates are the least constrained by observations and therefore most strongly influenced by the model physics (Rienecker et al., 2011), which, for convective precipitation especially, must be approximated using subgrid-scale parameterizations. This introduces considerable uncertainty into the MERRA precipitation. We therefore considered FWI System calculations using two other daily, global precipitation data sets that are based on rain gauge data. Sheffield et al. (2006) have produced global 1° × 1° fields of meteorological fields useful for land hydrology models. Their precipitation estimates start with monthly precipitation estimates from the University of East Anglia (UEA) Climatic Research Unit (CRU) monthly global gridded product (Mitchell and Jones, 2005) which are distributed at a daily frequency using National Centers for Environmental Prediction (NCEP)/National Center for Atmospheric Research (NCAR) reanalysis (Kalnay et al., 1996).

The National Oceanic and Atmospheric Administration (NOAA) Climate Prediction Center (CPC) produces estimates of global, daily precipitation fields over land from rain gauge data (Chen et al., 2008) at 0.5° × 0.5° resolution. Their optimal interpolation method makes use of the covariance structure of the precipitation field, which, compared to more simple distance-only-based interpolation methods, should improve estimates where orography is important. The accuracy of gauge-based estimates ultimately depends on the rain gauge density, which for our purpose was most sparse in northern Canada and Alaska, northern Russia, sub-Saharan Africa and equatorial Southeast Asia. The Sheffield and CPC precipitation fields will share much of the same raw data and should not be considered truly independent. The important differences in this context are in their approaches to interpolation over sparse regions and estimates at a daily time scale. In total, we produced three global FWI System data sets: MERRA only, MERRA with Sheffield (SHEFF) precipitation, and MERRA with CPC precipitation. Throughout the paper we refer to each FWI version by the name of the precipitation input.

Figure 1 shows the mean May snow depth and fraction of days over which the FWI System is active, based on our startup and shutdown procedures. The maps essentially show

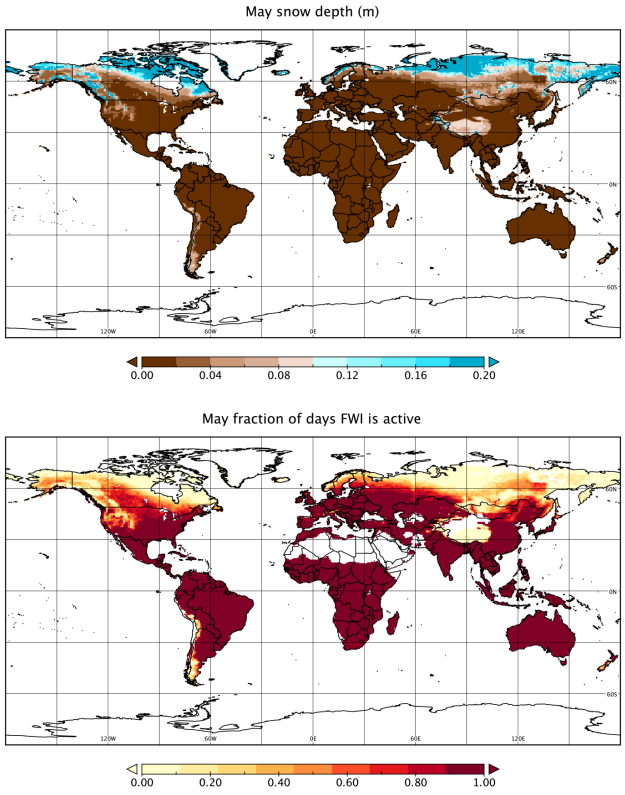

Figure 1. Mean MERRA snow depth (top) and fraction of active FWI calculation days (bottom) for May, 1980–2012. The fraction of active FWI calculation days refers to the number of days in May where DC calculations are not shut down due to cold conditions or snow cover.

the dependence and variability of FWI System startup on snow cover as the fire season is starting at higher latitudes in the Northern Hemisphere, in this case estimated from MERRA.

3.2 Station data

We compared the calculations from gridded data to those based on individual station data for a representative set of 48 stations obtained from a variety of sources (Table 2). Whenever possible, data were used that had previously been used by individual agencies for FWI System calculations. As such, the length of record varied by agency, as did the pre-processing procedures, which are described below. We sought pairs of stations in the same region to guard against localized effects and possible errors in single weather station records. Similar to the use of the two precipitation data sets, this is not a strict validation of the gridded FWI calculations per se, since some of the weather station data will have been assimilated into the MERRA analyses or the gridded precipitation fields. The comparison to station-based calculations instead provides a sense for users of the smoothing that occurs for grid-cell scale calculations. Individual station calculations were compared to the mean over the area defined by the station coordinates buffered by a 1/2° latitude and longitude band. Snow depth was generally not available for the station data and was instead sampled from the MERRA estimates. This also simplified our comparison by eliminating DMC and DC startup values as a potential difference between data sets.

Table 2 lists the stations used and the periods covered. The majority of stations were from World Meteorological Organization (WMO)-level synoptic stations and will therefore adhere somewhat to a common set of data quality standards. For consistency, comparison with the gridded FWI calculation was over the period of available data only for each individual station. Additional quality control and gap filling was applied following local procedures that we now describe.

Data for Canadian stations came from Environment Canada for the years 1979–1998, 1999 or 2006. Data were available only for the fire season, which was determined using a temperature threshold as outlined in Wotton and Flannigan (1993).

Data for stations in Thailand had no more than 3 % missing data for any of the input parameters. Missing data were interpolated temporally or spatially, and subject to established homogeneity tests for temperature and precipitation (Alexandersson, 1986; Manomaiphiboon et al., 2013). Wind siting was rated at least "fair" for all stations, indicating the absence of large barriers to unobstructed wind measurements.

For Australia, four pairs of stations were selected with each of these stations having no more than 0.7 % of days with missing data for any of the input parameters. Missing data for wind speed, relative humidity and temperature were replaced by the mean of the previous and subsequent days of available data, and missing data for precipitation were replaced by data from the nearby station (using the station pairs listed in Table 1). The rainfall data are for the 24 h period prior to 09:00 LT on the listed day. The four pairs of Australian stations have operated continuously throughout the study period (i.e., without being moved to a different location).

Data for Mexico and Guatemala were obtained from the Mexico Forest Fire Information System operated by the Canadian Forest Service at the Northern Forestry Centre. Weather data are collected in near real time from stations operated by the meteorological offices of the respective countries and supplying observations through the WMO's Global Observing Program and Global Telecommunications Service. The closest pairs of stations with the best observation records were chosen for this study, which were Mexicali and Tijuana in northwestern Mexico and Huehuetenango and Guatemala City Aurora in Guatemala.

When no direct agency FWI System input data were available in regions, we obtained raw hourly weather data directly from the NOAA National Climatic Data Center (NCDC) Integrated Surface Database (ISD) (Smith et al., 2011). In many cases for the ISD stations, there were large periods of missing data. Missing values were filled with those from MERRA for the sake of being able to continue the calculations. Periods with too much missing station data over an antecedent period, however, were excluded from our monthly climatological means and comparison. We required that 80 % of the previous 120 days had precipitation reporting for at least 18 h per day, similar to the requirement in Field et al. (2004) for their DC calculations over western Indonesia. This allowed us to make use of the precipitation reported as both daily and hourly totals, but with an effort to avoid introducing a systematic bias due to missing precipitation reports. The start and end years in Table 2 indicate the full period over which some data were available, but in most case the actual periods included when comparing the DC to the gridded data sets were much shorter, often only a few years. Stations in southern Europe tended to have higher quality from the mid-2000s onward, for example, whereas data from Indonesia was typically only of sufficient quality in the mid-1990s. The comparisons with the gridded calculations take this into account, but we therefore make comparisons between stations with a fair degree of caution. Information on data quality for the NCDC stations is provided as part of the GFWED data distribution.

4 Results

We used the Drought Code for our comparison between station and gridded calculations because it will most directly capture the sensitivity to different precipitation input data sets. In the following sections, we present DC comparisons for North America, Central and South America, northern Europe and Siberia, southern Europe, Thailand, Malaysia and

Table 2. Weather stations used for comparison to gridded calculations. Abbreviations are as follows: Environment Canada (EnvCan), Global Telecommunications System (GTS), Canadian Forest Service Northern Forestry Centre (NoFC), National Oceanic and Atmospheric Administration National Climatic Data Center (NCDC), Canadian Forest Service Great Lakes Forestry Centre (GLFC), Australian Bureau of Meteorology (BoM), Thailand Meteorology Department (TMD), Malaysian Meteorological Department (MMD). Environment Canada stations are specified by their agency identifiers and World Meteorological Organization (WMO) identifiers when available. All other stations are specified by their WMO identifiers. For the NCDC stations, data completeness and periods used in the analysis are provided as part of the data distribution.

ID	Name	Country	Lat.	Lon.	Source	Start year	End year
1123970 (71203)	Kelowna	Canada	49.88	−119.48	EnvCan	1980	2006
1126150 (71889)	Penticton	Canada	49.48	−119.58	EnvCan	1980	1998
5050960 (–)	Flin Flon	Canada	54.77	−101.85	EnvCan	1980	1999
5052880 71867	The Pas	Canada	53.82	−101.25	EnvCan	1980	1999
6072225 (–)	Earlton	Canada	47.71	−79.83	EnvCan	1980	1999
7098600 (71725)	Val-dOr	Canada	48.10	−77.78	EnvCan	1980	1995
760016	Mexicali	Mexico	32.63	−117.00	GTS-NoFC	1999	2012
760023	Tijuana	Mexico	32.55	−116.97	GTS-NoFC	1999	2012
786270	Huehuetenango	Guatemala	15.32	−91.47	GTS-NoFC	1999	2012
786410	Guatemala City	Guatemala	14.58	−90.52	GTS-NoFC	1999	2012
836120	Campo Grande	Brazil	−20.45	−54.72	NCDC	1980	2012
833620	Cuiaba	Brazil	−15.65	−56.10	NCDC	1980	2012
24600	Stockholm Arlanda	Sweden	59.65	17.95	GTS-NoFC	2001	2012
24640	Stockholm Bromma	Sweden	59.35	17.95	GTS-NoFC	2001	2012
29740	Helsinki Vantaa	Finland	61.32	24.97	GTS-NoFC	2004	2012
29750	Helsinki Malmi	Finland	61.25	25.05	GTS-NoFC	2001	2012
106160	Hahn	Germany	49.95	7.27	GTS-NoFC	2001	2012
107080	Saarbruecken	Germany	49.22	7.12	GTS-NoFC	2001	2012
286960	Kalachinsk	Russia	55.03	74.58	NCDC-GLFC	1980	2010
296360	Toguchin	Russia	55.23	84.40	NCDC-GLFC	1980	2010
80010	La Coruna	Spain	43.37	−8.42	NCDC	1980	2012
80420	Santiago	Spain	42.89	−8.41	NCDC	1980	2012
83910	Seville	Spain	37.42	−5.88	NCDC	1980	2012
84100	Cordoba	Spain	37.84	−4.85	NCDC	1980	2012
160880	Brescia	Italy	45.42	10.28	NCDC	1980	2012
160900	Verona	Italy	45.39	10.87	NCDC	1980	2012
166430	Aktion	Greece	38.62	20.77	NCDC	1980	2012
166820	Andravida	Greece	37.91	22.00	NCDC	1980	2012
483270	Chiang Mai	Thailand	18.77	98.97	TMD, NCDC	1980	2012
483030	Chiang Rai	Thailand	19.96	99.88	TMD, NCDC	1980	2012
484050	Roi Et	Thailand	16.12	103.77	TMD, NCDC	1980	2012
484070	Ubon Ratchathani	Thailand	15.25	104.87	TMD, NCDC	1980	2012
486500	Kuala Lumpur IA	Malaysia	3.08	101.65	MMD	2005	2012
486480	Petaling Jaya	Malaysia	3.08	101.65	MMD	2005	2012
964710	Kota Kinabalu	Malaysia	5.93	116.05	MMD	2004	2012
964910	Sandakan	Malaysia	5.25	118.00	MMD	2004	2012
962210	Palembang	Indonesia	−3.00	104.75	NCDC	1980	2012
962370	Pankalpinang	Indonesia	−3.00	104.75	NCDC	1980	2012
966550	Palangkaraya	Indonesia	−1.00	114.00	NCDC	1980	2012
966450	PangkalanBun	Indonesia	−2.70	111.70	NCDC	1980	2012
948650	Laverton	Australia	−37.86	144.76	BoM	1980	2012
948660	Melbourne	Australia	−37.67	144.83	BoM	1980	2012
942380	Tennant Creek	Australia	−19.64	134.18	BoM	1980	2012
943260	Alice Springs	Australia	−23.80	133.89	BoM	1980	2012
946380	Esperance	Australia	−33.83	121.89	BoM	1980	2012
946370	Kalgoorlie-Boulder	Australia	−30.78	121.45	BoM	1980	2012
947670	Sydney	Australia	−33.95	151.00	BoM	1980	2012
947760	Williamtown	Australia	−32.50	151.00	BoM	1980	2012

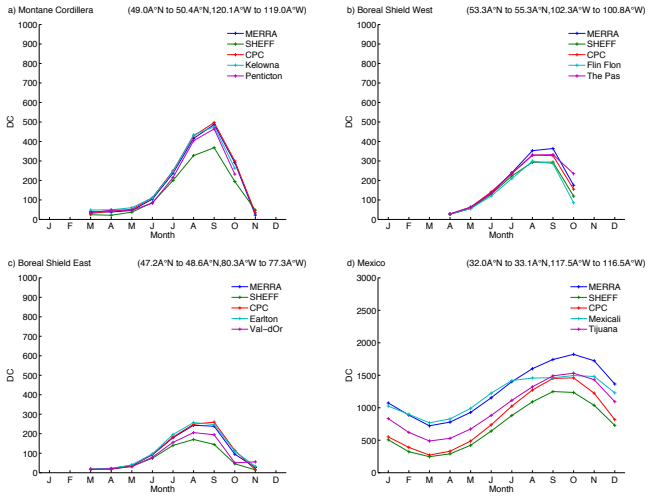

Figure 2. Monthly mean Drought Code (DC) for three regions in Canada and northwestern Mexico. MERRA, SHEFF and CPC DC are from the GFWED gridded fields over the latitude and longitude range specified in the caption. The other two DC plots are for representative weather stations in that range. Note the different DC scale for Mexico.

Indonesia and Australia. This is followed by a brief description of Global FWI patterns for January and June. For context, the regional descriptions include general characteristics of the fire environment, such as primary fuel types, timing of the fire season, and the number and size of fires. Comparisons in fire statistics should be interpreted only in the most general sense, and are only meaningful within a region. Mean fire size is a commonly reported statistic, but because frequency–size distributions can be highly non-normal (Millington et al., 2006; Cui and Perera, 2008), a mean fire size may not be a useful measure of center. Furthermore, reported means will be highly sensitive to the minimum reported fire size, which can vary across fire agencies, and over time as smaller and smaller fires are reported (Hincks et al., 2013). We hope in particular that the daily-resolution FWI fields provided as part of the GFWED data distribution will be useful in understanding the drivers of fire–size distributions in regions where detailed fire statistics are available.

4.1 North America

Figure 2 shows the monthly mean DC for three regions in Canada, for each of the three gridded data sets and two weather stations, and for northwestern Mexico. The southern British Columbia (BC) interior DC captures the southern, drier part of Canada's Montane Cordillera ecozone (Stocks et al., 2002). Fires in this region are numerous but tend to be smaller (Jiang et al., 2009), more often caused by humans and subject to intense fire management due to relatively high population density compared to other forested regions of the country. The DC values between the two stations are consistent for the station-based calculations, peaking in September with values approaching DC = 450 (Fig. 2a). The DC seasonality is captured well by the MERRA and CPC-based calculations, but has a low bias for the SHEFF precipitation, the DC for which peaks closer to DC = 350. Presumably this is because of the lower spatial resolution CRU/NCEP reanalysis-based estimates used in SHEFF and the influence of weather stations on the much wetter west coast.

Large (> 200 ha) fires occur most frequently in Canada in the Boreal Shield West ecozone (Stocks et al., 2002). Using our startup definition, the DC fire season starts in April (Fig. 2b), 1 month later than in British Columbia. Both stations are located in Manitoba, in the western portion of the ecozone. The DC peaks in August–September between DC = 250 and 300, reflecting the net drying that occurs in deeper fuels over the summer. The MERRA only-based DC (blue line) has a slightly higher bias than the SHEFF or CPC-based DC relative to the station-based calculations, but all gridded DC calculations peak within the DC = 300–425 danger class for that region during August and September, consistent with long-term CWFIS estimates. For reference, Amiro et al. (2004) determined that the maximum DC in this region calculated over days with large (> 200 ha) fires only was over DC = 400 during September. The lower DC values in the Boreal Shield East ecozone (Fig. 2c) compared to the Boreal Shield West values are consistent with a lower burned area. In the Boreal Shield West ecozone, an estimated 0.761 % percent of the forested area burns annually compared to 0.145 % in the Boreal Shield East ecozone (Stocks et al., 2002). This is presumably due to the influence of large-scale, cyclonic precipitation originating in the southern US which rarely arrives in the Boreal Shield West (Paciorek et al., 2002), and appears to have a slightly stronger influence on the Val-D'or station which is to the east of Earlton. The spread between the MERRA, SHEFF and CPC-based DC calculations is comparable to the differences between the two stations.

The stations in Mexico capture the DC conditions toward the southern extent of North America (Fig. 2d). Tijuana is a coastal city with a Mediterranean climate, separated by a low mountain range from Mexicali, which is on the western edge of the Sonoran desert. This arid environment has fuels similar to those found in the San Diego area in southern California (Minnich and Chou, 1997), consisting of areas of chaparral and grassland in the mountains and some broadleaf trees in the intermittent riparian zones. Fires are generally smaller on the Mexican side of the border compared to the Californian side, possibly in part due to differences in suppression programs (Minnich and Chou, 1997). Over 1920–1971, for example, the mean fire size in chamise chaparral of California was 921 ha compared to 101 ha for the same vegetation type in Mexico (Minnich and Chou, 1997). Due to the aridity of this environment, DC values routinely exceed DC = 1000 and often reach DC = 1500 in the hottest and driest summer periods. During the wetter seasons, the

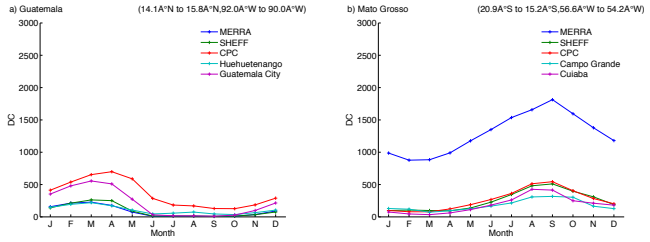

Figure 3. Monthly mean DC for Guatemala and the Mato Grosso of Brazil. MERRA, SHEFF and CPC DC are from the GFWED gridded fields over the latitude and longitude range specified in the caption. The other two DC plots are for representative weather stations in that range.

DC values are usually reduced to the DC = 700–800 range in Mexicali and DC = 300–500 in the coastal Tijuana area, with the lower values in Tijuana presumably due to influence of winter precipitation at its coastal location. The absence of winter snow or a strong wet season means that, on average, deep fuel moisture does not fully recharge and the DC does not "zero-out". The MERRA data generally has the highest DC values, although all model variations closely follow the DC trends in the hot and dry late summer and early autumn period. The CPC and SHEFF DC are lower than either station during the spring.

4.2 Central and South America

The stations in Guatemala capture seasonally wet conditions in Central America (Fig. 3a). Huehuetenango and Guatemala City fall in the Tropical Mountain ecological zone at similar elevations roughly 100 km inland from the Pacific Ocean. Trees are diverse and include oak, cypress, pine and fir (Veblen, 1978). Most fires appear to be human-caused due to agricultural slash and burn practices or escaped trash burns (Monzón-Alvarado et al., 2012). The fire problem intensifies with deadfall left from pine beetle infestations (Billings et al., 2004). About 90 % of the annual rain falls between May and October, with slightly higher temperatures during the dry season from February through June. Based on the CPC precipitation estimate, the Huehuetenango area receives slightly more annual precipitation (∼ 1570 mm), with an increasing gradient up the escarpment to the north, than Guatemala City (∼ 1130 mm). The DC should therefore range from high winter values to near-zero through the summer and early fall. This trend is shown by the station and gridded data, with the mean March DC approaching DC = 500 at Guatemala City at the end of the dry season. MERRA and SHEFF DC generally fall in between the two stations during the entire year. The CPC DC is consistently higher than the drier Guatemala City DC. This difference is greatest during May and June, perhaps because the CPC data are not capturing spotty, convective precipitation during the onset of the monsoon.

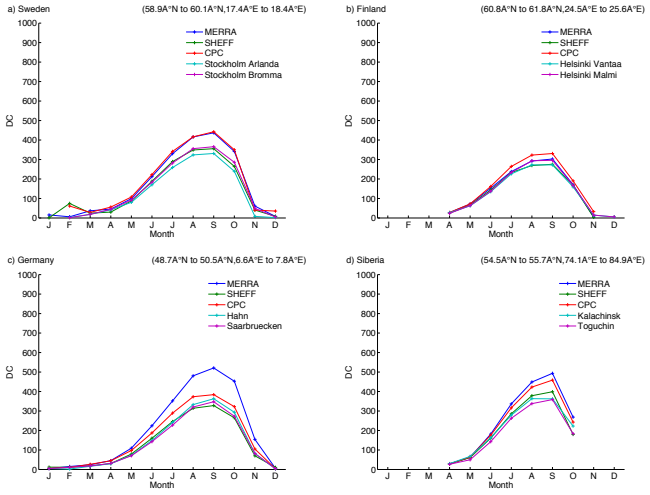

Figure 4. Monthly mean DC for northern Europe and Siberia. MERRA, SHEFF and CPC DC are from the GFWED gridded fields over the latitude and longitude range specified in the caption. The other two DC plots are for representative weather stations in that range.

The Brazilian Mato Grosso is an important region of seasonal fire activity resulting from agricultural burning (Morton et al., 2013). The peak DC approaching DC = 500 (Fig. 3b) is similar to the Guatemalan stations, but with opposite seasonality, peaking in August and September at the end of the dry season. The SHEFF and CPC DC are in close agreement with the station data. The MERRA DC, however, has an extremely high bias, reaching peak DC = 1500 and a minimum of DC = 750. This reflects a strong low precipitation bias in the MERRA precipitation relative to gauge-based estimates (Lorenz and Kunstmann, 2012) that is strong enough to maintain extreme DC throughout the year.

4.3 Northern Europe and Siberia

The DC seasonality of the boreal forest region in northern Europe and Siberia (Fig. 4) is similar to those of the Canadian boreal region, the Boreal Shield West (Fig. 2b) especially. Peak DC values occur in September after most seasonal fuel drying has occurred and decreases as autumn progresses with decreasing environmental drying conditions. The fire season in Siberia ends in October (Fig. 4d), earlier than the other regions, due to the earlier arrival of snow. Although the range of fire weather conditions in northern boreal Eurasia is similar to boreal North America, the continental fire regimes have important differences (de Groot et al., 2013a). In comparing large fire characteristics, those in boreal North America had a mean size of 5930 ha compared to 1312 ha in boreal Russia, but a fire return interval of 179.9 years compared to 52.9 years in boreal Russia (de Groot et al., 2013a). Divergent continental boreal fire regimes are attributed to differences in tree species even though *Picea, Pinus, Larix, Abies,*

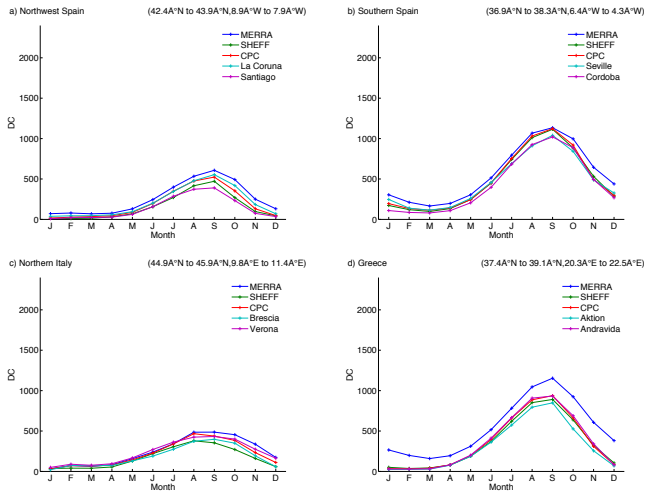

Figure 5. Monthly mean DC for four regions in southern Europe. MERRA, SHEFF and CPC DC are from the GFWED gridded fields over the latitude and longitude range specified in the caption. The other two DC plots are for representative weather stations in that range.

Populus and *Betula* spp. occur throughout the circumpolar boreal region (de Groot et al., 2013b). The boreal fire regime of northern Europe and Russia east of the Urals is similar to the southern boreal of Canada with many fires being human-caused but small in size due to population size, extensive suppression capacity and road access (Lehsten et al., 2014). There is generally fair agreement between the data sets, save for anomalously high peak MERRA DC over Germany (Fig. 4c), which is consistent with Lorenz and Kunstmann's (2012) identification of lower precipitation over Central Europe in MERRA relative to gauge-based data sets.

4.4 Southern Europe

The stations in northwestern Spain and northern Italy form a transect across the northern Mediterranean and the stations in southern Spain and Greece across the southern Mediterranean (Fig. 5). In the Mediterranean the DC does not reflect the moisture conditions of deep soil organic layers, as soils are typically poor and a deep organic layer is normally absent (Chelli et al., 2014). Instead, we interpret the DC as a general indicator of seasonal drying. Some studies found DC to correlate with live fuel moisture content of Mediterranean shrubs (e.g., Castro et al., 2003; Pellizzaro et al., 2007; Chelli et al., 2014). There, increases in DC above 600–800 are likely not reflecting an actual increase in fire danger because the fuels have become as dry as possible. This is also likely the case in other semi-arid regions.

Northwestern Spain has a marked Atlantic climate with the highest precipitation amount in the Iberian Peninsula. Atmospheric circulation in the summer is highly variable, alternating between strong dry and humid periods (Diez, 1993). It is one of the more fire-prone regions in Spain (Padilla and Vega-Garcia, 2011) with ∼ 6000 fires per year, typically concentrated during short dry summer periods. The total burned area is ∼ 30 000 ha per year, but the mean fire size of 4.9 ha is less than in the rest of Spain (7.6 ha) due to aggressive suppression policy (Padilla and Vega-Garcia, 2011). Extremely large (> 500 ha) fires constitute only 0.13 % of all fires, but fire-fighting agencies are often challenged by many fires burning at the same time (Padilla and Vega-Garcia, 2011). Fire occurrence patterns are affected more by human activities than by biophysical characteristics of the fire environment (Padilla and Vega-Garcia, 2011), but there is an August peak in fire activity. The DC peaks in September (Fig. 5a), and is higher at La Coruna (DC = 500) on the coast, compared to Santiago located 50 km inland. The CPC and SHEFF DC fall in between the two stations, with MERRA being slightly higher throughout the year.

The stations in southern Spain capture a typical inland Mediterranean climate with dry hot summers. The vegetation is dominated by a mosaic of shrublands and low forests with frequent crown fires (Keeley et al., 2011). Although this is a fire-prone area and large fires may occur, fire activity is less remarkable than in other Mediterranean regions (Pausas and Paula, 2012) with 900 fires each year, having a mean size of 13.5 ha and total annual average burned area of 12 000 ha. In the extremely dry climatic condition of the area, fuel structure tends to be more relevant in driving fire activity than the frequency of climatic conditions conducive to fire (Pausas and Paula, 2012). Wildfires are more fuel-limited and more extreme climatic conditions (higher aridity than in more mesic regions) are needed for fires to spread successfully (Pausas and Paula, 2012). The peak of the fire season is typically in June, July, August, corresponding to values between DC = 500 and 1000 (Fig. 5b). The DC seasonality and magnitude at the Seville and Cordoba stations are essentially identical, with both stations in the low-lying Guadalquivir river basin. All gridded data slightly overestimate DC in summer months, and the MERRA DC is slightly higher throughout the year.

The stations in northern Italy south of the Alps reflect a sub-continental temperate climate, with predominantly deciduous broadleaved forest (Zumbrunnen et al., 2009; Wastl et al., 2013). The peak of the fire activity is in March–April, after snowmelt and before leaf flushing. Population, vegetation phenology and short-term dryness of surface soil layers often triggered by Foehn winds off the Alps are the main drivers, rather than long term DC. Fires in this region are on average small, with mean fire size ∼ 2 ha and 98 % of fires smaller than 10 ha, and rarely achieve crown involvement (Zumbrunnen et al., 2009; Wastl et al., 2013). The station and gridded data are all similar, peaking at the end of the summer near DC = 500 (Fig. 5c).

The stations in Greece reflect a Mediterranean climate, but one was less arid than southern Spain and one had severe fire incidence and frequent large fires during the summer. 1.2 %

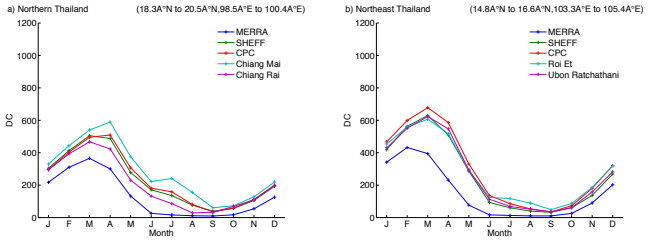

Figure 6. Monthly mean DC for two regions in Thailand. MERRA, SHEFF and CPC DC are from the GFWED gridded fields over the latitude and longitude range specified in the caption. The other two DC plots are for representative weather stations in that range.

of fires are larger than 500 ha and the average fire size is 45 ha. DC peaks in August–September with extremely high values approaching DC = 1000, slightly lower at Aktion due to its coastal location, 100 km to the north (Fig. 5d). SHEFF and CPC are in good agreement with Andravida weather station and MERRA has a high DC bias throughout the year. Seasonal drought is an important driver of fire activity in the area, but as in the rest of the Mediterranean region, the deep organic layer of soil is absent in most cases, thus DC reflects seasonal drying rather than moisture content of deep organic fuels. Significant relationships of monthly burned area and FWI components (DC and ISI), were found for the Mediterranean region (Camia and Amatulli, 2009) and for individual southern European countries including Greece (Amatulli et al., 2013).

4.5 Thailand

The fire season in Thailand is from early December to early May during the southward displacement of the Intertropical Convergence Zone (ITCZ) (Tanpipat et al., 2009; Chien et al., 2011). Fires are usually human-caused for the purposes of gathering non-timber products, hunting and agriculture, and occur primarily in the afternoon (Tanpipat et al., 2009; Chien et al., 2011). Thailand is an important region for possible FWI System use, given the persistence of its fire and haze problem and the expanding role of the Association of Southeast Asian Nations (ASEAN) for fire management, to which the FWI System is central (de Groot et al., 2007).

Figure 6 shows monthly mean DC for two regions in Thailand. Biomass burning is the dominant emissions source for particulate matter in northern Thailand (Nguyen and Leelasakultum, 2011), which experiences periodically severe haze as a result. The DC peaks in March and April near DC = 500 at both stations, followed by the end of the dry season (Fig. 6a). In Chiang Mai, there is also a secondary dry period in July, but its absence in Chiang Rai suggests local effects or artifacts of input data common to both gridded precipitation data sets. The minimum DC in both locations occurs in the August to September period during the height of the Asian summer monsoon. The SHEFF and CPC-based DC are in good agreement with station data for both locations, both falling between the two stations during most of the year. There is a strong low DC bias in the MERRA data set throughout the year. The DC in northeast Thailand (Fig. 6b) has roughly the same seasonality, but with a higher March peak of DC = 600. The CPC, SHEFF and station-based DC are all in strong agreement, and the MERRA-based DC again shows a low bias. Compared to northern Thailand, there is a smaller difference between the two stations in the northeast, which we attribute to the region's uniform topography.

4.6 Malaysia and Indonesia

The stations in Malaysia and Indonesia are representative of the equatorial Southeast Asia fire region identified by van der Werf et al. (2010). Fire activity in southern Sumatra and southern Kalimantan is higher than in Sabah or Peninsular Malaysia (van der Werf et al., 2008; Langner and Siegert, 2009; Giglio et al., 2013). On the average, close to 5 % of these Indonesian regions burn per year, while the comparable statistic for these Malaysian regions is less than 0.3 % (Giglio et al., 2013). This is due to greater forest loss over the past two decades in Indonesia, principally due to deforestation fires for establishing palm oil, timber and pulp paper plantations, as well as escaped fires linked to illegal logging activities (Langner and Siegert, 2009; Mukherjee and Sovacool, 2014). These fires have left many areas with highly degraded forests that are prone to even more fires, especially during El-Niño events (Hoscilo et al., 2011). These problems are mitigated in Malaysia to some extent by more active monitoring, regulation and enforcement by government authorities and fire suppression (Langner and Siegert, 2009; Forsyth, 2014; Mukherjee and Sovacool, 2014) compared with Indonesia. The fire seasons in the region are controlled by rainfall seasonality. Different regions of Indonesia and Malaysia have an annual wet–dry cycle, a semi-annual cycle or have no clear wet and dry cycles (Aldrian and Susanto, 2003). In southern Sumatra and southern Kalimantan, the monsoon consists of two distinct phases with the wet season occurring in the early part of the year (January–March) and the dry season in the middle of the year (July–September) (Aldrian and Susanto, 2003).

The seasonal DC patterns for Peninsular Malaysia, Sabah, southern Sumatra, and southern Kalimantan (Fig. 7) reflect these rainfall patterns. Southern Sumatra has the strongest DC seasonality (Fig. 7c); the longer dry season allows mean DC approaching DC = 300 to be reached in September. The timing and magnitude are well captured by the SHEFF and CPC data sets, but a wet MERRA bias results in lower DC. The seasonality in southern Kalimantan is similar (Fig. 7d), but on average, the peak DC of DC = 200 is lower than Sumatra.

The DC seasonality in Malaysia is less consistent than Indonesia. In Peninsular Malaysia (Fig. 7a), both stations have a July peak, but which is higher at KLIA compared

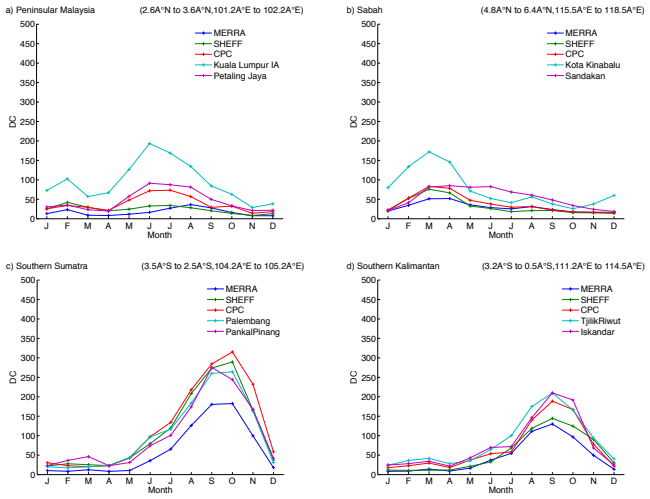

Figure 7. Monthly mean DC for two regions in each of Malaysia and Indonesia. MERRA, SHEFF and CPC DC are from the GFWED gridded fields over the latitude and longitude range specified in the caption. The other two DC plots are for representative weather stations in that range.

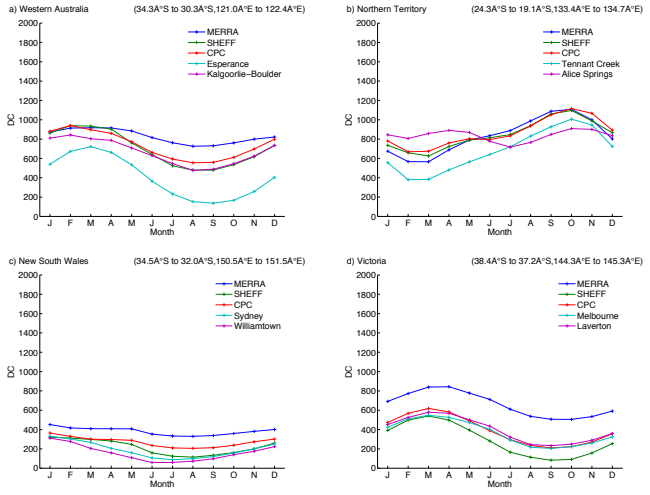

Figure 8. Monthly mean DC for four regions in Australia. MERRA, SHEFF and CPC DC are from the GFWED gridded fields over the latitude and longitude range specified in the caption. The other two DC plots are for representative weather stations in that range.

to Petaling Jaya, perhaps reflecting localized effects. The CPC DC corresponds closely to that in Petaling Jaya, and MERRA has very little seasonality. In Sabah (Fig. 7b), there is a strong DC seasonality in Kota Kinabalu, but not in Sandakan. The difference is likely due to complex air–sea interaction and topography, with the two stations separated by the Crocker mountain range. The more complicated seasonality in Malaysia reflects the fact that it falls outside of the distinct rainfall zone identified by Aldrian and Susanto (2003). We note, however, that the apparently strong differences between data sets reflect a narrower DC scale and should not be over-interpreted.

El-Niño-induced droughts are a recurrent feature of the region, and hence, inter-annual variability in rainfall across the regions is high (van der Werf et al., 2008; Field and Shen, 2008; Field et al., 2009; Spessa et al., 2015). As such, there is considerable variation surrounding the long-term mean monthly DC values shown in Fig. 7. Field et al. (2004) estimated that the severe fire episodes in 1994 and 1997 in Sumatra and Kalimantan were associated with DC greater than DC = 400. During non-El Nino years, and on average, this DC threshold is not reached and heavy fuels, especially peat, remain too moist to burn.

Viewed regionally across Southeast Asia, the DC seasonality in Thailand (Fig. 6a, b) is opposite that of Indonesia (Fig. 7c, d), with Malaysia (Fig. 7a, b) falling in between. MERRA-derived DC is consistently lower than all DC products in all regions, especially during the dry season. This is similar to Thailand, and consistent with previous work showing that MERRA has a wet bias in Southeast Asia relative to gauge-based estimates (Lorenz and Kunstmann, 2012).

4.7 Australia

Monthly mean DC values are shown in Fig. 8 for four regions in Australia. In Western Australia (Fig. 8a), the seasonal cycle of the DC values based on the gridded data is similar to that of the station-based data, in that maximum values occur during the warmer months and the minimum values during the cooler months. The DC values based on the Esperance station data are lower than those based on the Kalgoorlie-Boulder station data, with a maximum approaching DC = 700 in March and a minimum of DC = 100 in September. This is consistent with Esperance being located nearer to the coast with a cooler and wetter climate than Kalgoorlie-Boulder, where the August minimum is DC = 500. The DC values based on the gridded data are similar in magnitude to those based on the more inland station (Kalgoorlie-Boulder), with DC values based on SHEFF and CPC data being highly consistent throughout the year with the Kalgoorlie-Boulder station-based data. The DC values based on MERRA are somewhat higher than the Kalgoorlie-Boulder station-based data during the cooler months of the year, and relatively similar to the other two gridded data sets during the warmer months of the year.

In the Northern Territory (Fig. 8b), the DC values based on the Tennant Creek station data have a maximum approaching DC = 1000 during spring (from about September to November) corresponding to the later part of the tropical dry season in the Southern Hemisphere. The DC values based on the Alice Springs station data have a less pronounced seasonal cycle than the case for Tennant Creek, due to Alice Springs being located somewhat further south and having a more temperate climate than Tennant Creek. The DC values based on the gridded data have magnitudes broadly similar

to the station-based data with a seasonal cycle similar to the case for Tennant Creek (i.e., a more pronounced spring maximum than the case for Alice Springs). There is little variation between the three gridded data sets for any month of the year.

In New South Wales (Fig. 8c), the gridded data are consistent with the station data in having maximum DC values during the warmer months of the year. The DC values based on the gridded data tend to be larger in magnitude than those based on the station data. This is consistent with the gridded data representing the mean conditions throughout a grid cell, whereas the two stations are both located very close to the coast and have relatively moderate temperatures and high rainfall as compared to nearby inland regions.

In Victoria (Fig. 8d), the DC values based on the data from the two stations are very similar to each other throughout the year, peaking at DC = 600 in March. These stations are located relatively close to each other and both have strong maritime influences on their climate. The DC values based on the SHEFF and CPC data are almost identical to those based on the station data for all months of the year. The DC values based on MERRA data capture the seasonal cycle, but are consistently higher by DC = 200.

Regional fire activity in Australia broadly follows the timing of the seasonal cycle of DC values shown in Fig. 8. In Victoria, fire activity predominantly occurs during the warmer months of the year, with a peak in fire activity around the later parts of summer from about January to March, while noting that occasional serious fires are likely to occur anytime from about November to April (Luke and McArthur, 1978; Russell-Smith et al., 2007). For example, the fire affected region during the January to March period is on average about 0.41 % of the southeastern mesic region of Australia, compared with only about 0.03 % from April to June, 0.05 % from July to September and 0.11 % from October to December (Russell-Smith et al., 2007). The DC values for the Victorian stations peak from February to April, indicating considerable overlap with the period of peak fire activity in this region, as well as a tendency towards a time lag of about 1 month compared to the timing of fire activity. This time lag could be expected to some degree, given that the fuel drying speed indicated by the DC is about 52 days (i.e., the time to lose about two thirds of its free moisture above equilibrium), as compared to about 12 days for the DMC and 2/3 of a day for the FFMC, with the FFMC and DMC also being important indicators of severe fire weather conditions in Australia in addition to the DC (Dowdy et al., 2010).

4.8 Summary of DC comparisons

Over northern latitudes with winter shutdown (Montane Cordillera, Boreal Shield West, Boreal Shield East, Sweden, Finland, Germany and Siberia), DC peaks in August and September between DC = 200 and 500. Mediterranean regions showed the same seasonality, but in southern Spain and Greece, the hottest regions considered, values exceeded DC = 1000 depending on the data set. DC values across data sets diverged over the course of the summer from similar, low startup values, but no systematic differences were apparent across different data sets, except perhaps that the DC calculations based on SHEFF had lower peak values in the Montane Cordillera, east Boreal Shield and Sweden and Siberia.

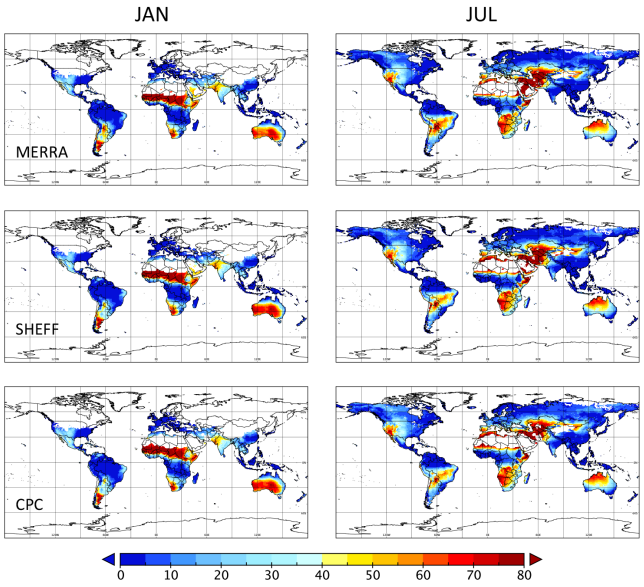

Figure 9. Global gridded mean FWI for January and July based on MERRA precipitation (1980–2012), Sheffield precipitation (1980–2008) and CPC precipitation (1980–2012).

Regions in Australia exhibited the weakest DC seasonality. In Western Australia and the Northern Territory, values ranged between DC = 500 and 1000, never, on average, "bottoming-out". DC values were lower in New South Wales and Victoria, but also not, on average, reaching 0, which was the case for the two stations presumably due to their coastal location.

Guatemala, the Brazilian Mato Grosso and Thailand have the strongest wet–dry seasonality. Excluding MERRA, DC peaked between DC = 400 and 600 and approached 0 during the wet season. The lowest overall values were in equatorial Southeast Asia which lacks as pronounced a dry season. The Malaysian regions lacked pronounced seasonal maxima and the gridded products never exceeded seasonal means of DC = 100. The Indonesian regions had a greater seasonality, but with seasonal peaks of less than DC = 300. As stated above, this seasonal average masks strong interannual variability.

4.9 Global FWI variability

Figure 9 shows the mean global Fire Weather Index (FWI) during January and July for all three data sets. The mean FWI is calculated from 1980–2012, excluding 1979 as a moisture code equilibration year. We describe FWI season-

ality according to selected fire regions defined by van der Werf et al. (2010), starting with the MERRA-based calculations. In January, FWI calculations are not active over the boreal North America and boreal Asia regions. Over temperate North America and Europe, mean FWI values reflect only a small number of anomalous warm and snow-free days during which the calculations were active. At low latitudes, the highest values based on MERRA are over northern hemispheric Africa, which contributes significantly to global emissions, when the ITCZ is displaced to the south. FWI is also high (> 40) in areas of southern hemispheric South America, the southern half of Australia, excepting its eastern coast, and northwest India. There are moderate (20–40) FWI values in Mexico and parts of continental Southeast Asia. Elsewhere, the FWI is generally low, including over the Amazon basin, northern hemispheric South America, the Congo basin, and equatorial Southeast Asia.

In June, the FWI System is active over the northern boreal regions, and does generally not exceed 30. Although an FWI of 30 is well below the seasonal peak at low latitudes, this can reflect severe fire danger conditions over the boreal regions (see, for example, the FWI categorical classification for the CWFIS, http://cwfis.nrcan.gc.ca). In the northern temperate regions, high values are seen over the fire-prone regions of the western US (approaching 50) and the Mediterranean. The extremely high FWI over northern hemispheric Africa has mostly been replaced by low FWI during the wet season and onset of the West African monsoon. By July, the dry season in equatorial Southeast Asia has just started and FWI values are still low. High FWI values are seen in southern hemispheric South America, corresponding, for example, to the active fire season in the Brazilian Mato Grosso (Chen et al., 2011; Fernandes et al., 2011), with comparable increases over southern Africa and northern Australia, all corresponding to the northward shift of the ITCZ.

In Australia, the three gridded data sets show strong similarities to each other in most regions during January and July. The highest FWI values during January tend to occur in the southern and southwestern regions, due to the dry and hot summer conditions of the temperate climate, while during July the highest values occur in the northern regions corresponding to the tropical dry season. The FWI values in eastern Australia are generally not as high as in other parts of mainland Australia, consistent with previous studies based on numerical weather prediction (NWP) analyses (Dowdy et al., 2010), relating to the significant maritime influences that occur in this region (e.g., trade wind transport of moist air inland from the Pacific Ocean).

Viewed globally, there is strong agreement between the three data sets. All major seasonal differences in the MERRA FWI are present in the SHEFF and CPC FWI. In January, the strongest difference was over central South America, where SHEFF and in particular CPC FWI were much lower than MERRA. This is consistent with the strong low precipitation bias in MERRA over the region identified by Lorenz and Kunstmann (2012), and effect on the DC described previously. SHEFF and CPC FWI are higher over Mexico, northern hemispheric Africa, continental Southeast Asia and northern Australia. In June, the higher MERRA values persist, but with an eastward shift. Sheffield and CPC FWI tended to be higher over the southeast US, East Africa and southern India.

The consistency in the differences between MERRA and the two gauge-based FWI calculations reflects the common station data used in computing the latter two. Whether or not the gauge-based calculations are better will ultimately depend on the underlying rain gauge density (Lawson and Armitage, 2008). This information was available for the CPC precipitation data set, shown in Fig. 10 during the 1979–2012

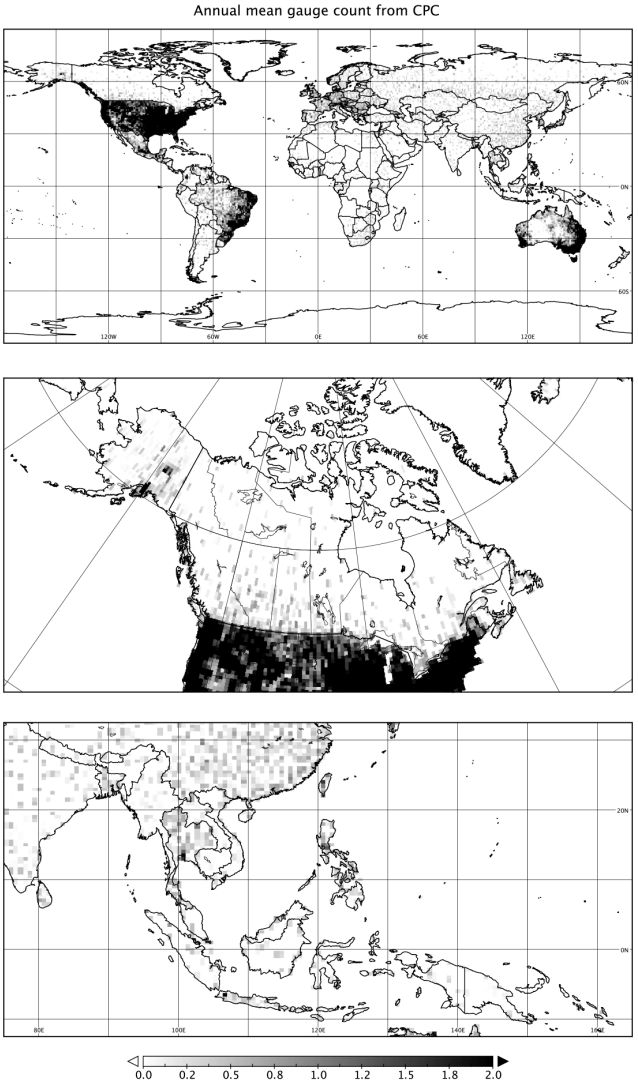

Figure 10. Mean 1979–2012 CPC rain gauge coverage (gauges/grid cell) for the globe (top), Canada (middle), Southeast Asia (bottom). The number of active rain gauges can change significantly from year to year. This information is provided as part of the data distribution.

period. Values less than 1 indicate stations not operating during the full analysis period. Users are encouraged to consider rain gauge density for any region over which analyses are performed.

Globally, gauge density is highest over the US, eastern Brazil and the populated coastal regions of Australia (Fig. 10). Density is reasonably high over central South America, which suggests that the low bias in the MERRA precipitation is genuine and that the MERRA FWI values there are unreliable. This is likely the case for MERRA's high precipitation and low FWI biases over continental Southeast Asia also, or for Thailand at least, where the CPC station density is high. In the northern boreal region, coverage is sparse but fairly even across fire-prone areas. In Southeast Asia, rain gauge density is low over the severe burning regions of Borneo and Sumatra. This limits spatially detailed FWI analysis over the region, although previous analyses have shown that precipitation covariance over the region is strong enough (Aldrian and Susanto, 2003) that the FWI System values should provide useful information at a provincial or state level. Identifying a more appropriate FWI version over tropical Africa is difficult due to the sparse and uneven gauge distribution, as cautioned by Chen et al. (2008) for precipitation-based analyses in general.

5 Summary

We have developed a global database of the Canadian FWI System components using MERRA reanalysis and two different gauge-based precipitation data sets. This data set can be used for historical relationships between fire weather and fire activity at continental and global scales, in identifying large-scale atmosphere–ocean controls on fire weather, calibration of FWI-based fire prediction models, and as a baseline for projections of fire weather under future climate scenarios as the reanalysis products improve.

Compared to the station-based calculation, the strongest differences between the three data sets occurred for the MERRA-based DC calculations at low latitudes. These biases were in either direction: over the Mato-Grosso peak dry season DC was higher than station or gridded rain gauge calculations by a factor of 3 (Fig. 3b), but,conversely had a low bias over Southeast Asia (Figs. 6, 7). We attribute these biases to the inherent difficulty in modeling convective precipitation, which remains a central challenge to numerical weather and climate modeling (Arakawa, 2004), and has disproportionate effects over the tropics. Temperature, wind and humidity discrepancies could also contribute to the differences between gridded and station-based calculations, particularly over regions with significant topography. While we have examined only one reanalysis-based product, we argue that FWI System calculations based solely on reanalysis products will be subject to the same discrepancies, and that alternative precipitation estimates are important to consider. Users are encouraged to conduct analyses over all three precipitation-based data sets in GFWED.

In the future, we hope to increase the number of versions using other input data sets, for example, other state-of-the-art reanalyses or satellite-based precipitation estimates such as the Global Precipitation Climatology Project (GPCP) (Huffman et al., 2009), Tropical Rainfall Measuring Mission (TRMM) (Huffman et al., 2007) and Global Precipitation Measurement (GPM) (Smith et al., 2007) mission. There is also the potential to compute the moisture codes using new soil moisture retrievals from the Soil Moisture and Ocean Salinity Mission (SMOS) (Kerr et al., 2010) and Soil Moisture Active Passive (SMAP) (Entekhabi et al., 2010) mission. The data sets could also be extended to include other weather-based fire danger indices such as the Nesterov Index, which continues to be used operationally and for research purposes (Thonicke et al., 2010) the McArthur Forest Fire Danger Index (McArthur, 1967; Noble et al., 1980), and, to capture the influence of atmospheric instability, the Haines Index (Haines, 1988). In regions with seasonal snow cover, different moisture code startup procedures and snow cover estimates should be examined, ideally taking into account local land cover and topographic characteristics as described in Lawson and Armitage (2008). We hope that users of the data continue to compare gridded fire weather calculations against those from weather stations, particularly for regions not considered here, and from secondary meteorological networks not used in any of the MERRA, Sheffield or CPC data sets. We also encourage comparison for components other than the DC, especially the ISI and FWI which are strongly influenced by surface winds.

Acknowledgements. We thank José Moreno and an anonymous reviewer for their short comment and detailed review, respectively. We thank Steve Taylor for his review and for identifying and pointing out the error in DMC lag times. VT and KM thank the Thailand Meteorological Department for providing weather data, and Prayoonyong Nhuchaiya for guidance. AD was supported by the Australian Climate Change Science Program (ACCSP). AS was supported by the Open University Research Investment Fellowship scheme. Resources supporting this work were provided by the NASA High-End Computing (HEC) Program through the NASA Center for Climate Simulation (NCCS) at the Goddard Space Flight Center. All data and code used in generating GFWED can be obtained from http://data.giss.nasa.gov/impacts/gfwed/.

Edited by: B. D. Malamud
Reviewed by: S. W. Taylor and one anonymous referee

References

Aldrian, E. and Susanto, R. D.: Identification of three dominant rainfall regions within Indonesia and their relationship to sea surface temperature, Int. J. Climatol., 23, 1435–1452, doi:10.1002/joc.950, 2003.

Alexandersson, H.: A homogeneity test applied to precipitation data, J. Climatol., 6, 661–675, 1986.

Amatulli, G., Camia, A., and San-Miguel-Ayanz, J.: Estimating future burned areas under changing climate in the EU-Mediterranean countries, Sci. Total Environ., 450, 209–222, doi:10.1016/j.scitotenv.2013.02.014, 2013.

Amiro, B. D., Logan, K. A., Wotton, B. M., Flannigan, M. D., Todd, J. B., Stocks, B. J., and Martell, D. L.: Fire weather index system components for large fires in the Canadian boreal forest, Int. J. Wildland Fire, 13, 391–400, doi:10.1071/wf03066, 2004.

Arakawa, A.: The cumulus parameterization problem: Past, present, and future, J. Climate, 17, 2493–2525, doi:10.1175/1520-0442(2004)017<2493:ratcpp> 2.0.co;2, 2004.

Bedia, J., Herrera, S., Gutiérrez, J. M., Zavala, G., Urbieta, I. R., and Moreno, J. M.: Sensitivity of fire weather index to different reanalysis products in the Iberian Peninsula, Nat. Hazards Earth Syst. Sci., 12, 699–708, doi:10.5194/nhess-12-699-2012, 2012.

Billings, R. F., Clarke, S. R., Espino Mendoza, V., Cordón Cabrera, P., Meléndez Figueroa, B., Ramón Campos, J., and Baeza, G.: Bark beetle outbreaks and fire: A devastating combination for Central America's pine forests, Unasylva, 55, 15–18, 2004.

Camia, A. and Amatulli, G.: Weather Factors and Fire Danger in the Mediterranean, in Earth Observation of Wildland Fires in Mediterranean Ecosystems, edited by: Chuvieco, E., 71–82, Springer-Verlag, Berlin, doi:10.1007/978-3-642-01754-4_6, 2009.

Camia, A. and Amatulli, G.: Climatology of FWI over Europe: fire danger anomalies and index percentiles rankings, in VI International Conference on Forest Fire Research, edited by: Viegas, D., p. 12, Coimbra, Portugal, 2010.

Castro, F. X., Tudela, A., and Sebastia, M. T.: Modeling moisture content in shrubs to predict fire risk in Catalonia (Spain), Agr. Forest Meteorol., 116, 49–59, doi:10.1016/s0168-1923(02)00248-4, 2003.

Chelli, S., Maponi, P., Campetella, G., Monteverde, P., Foglia, M., Paris, E., Lolis, A., and Panagopoulos, T.: Adaptation of the Canadian Fire Weather Index to Mediterranean Forests, Nat. Hazards, 1–16, doi:10.1007/s11069-014-1397-8, 2014.

Chen, M. Y., Shi, W., Xie, P. P., Silva, V. B. S., Kousky, V. E., Higgins, R. W., and Janowiak, J. E.: Assessing objective techniques for gauge-based analyses of global daily precipitation, J. Geophys. Res., 113, D04110, doi:10.1029/2007JD009132, 2008.

Chen, Y., Randerson, J. T., Morton, D. C., DeFries, R. S., Collatz, G. J., Kasibhatla, P. S., Giglio, L., Jin, Y., and Marlier, M. E.: Forecasting Fire Season Severity in South America Using Sea Surface Temperature Anomalies, Science, 334, 787–791, doi:10.1126/science.1209472, 2011.

Chien, S., Doubleday, J., McLaren, D., Davies, A., Tran, D., Tanpipat, V., Akaakara, S., Ratanasuwan, A., and Mandl, D.: Space-based sensorweb monitoring of wildfires in Thailand, 2011 IEEE International Geoscience and Remote Sensing Symposium (IGARSS), 1906–1909, 2011.

Chu, T. and Guo, X.: An assessment of fire occurrence regime and performance of Canadian fire weather index in south central Siberian boreal region, Nat. Hazards Earth Syst. Sci. Discuss., 2, 4711–4742, doi:10.5194/nhessd-2-4711-2014, 2014.

Cui, W. and Perera, A. H.: What do we know about forest fire size distribution, and why is this knowledge useful for forest management?, Int. J. Wildland Fire, 17, 234–244, doi:10.1071/wf06145, 2008.

de Groot, W. J., Cantin, A. S., Flannigan, M. D., Soja, A. J., Gowman, L. M., and Newbery, A.: A comparison of Canadian and Russian boreal forest fire regimes, Forest Ecol. Manage., 294, 23–34, doi:10.1016/j.foreco.2012.07.033, 2013a.

de Groot, W. J. and Flannigan, M. D.: Climate Change and Early Warning Systems for Wildland Fire, in: Reducing Disaster: Early Warning S ystems for Climate Change, edited by: Zommers, Z. and Singh, A., 127–151, Springer, Dordrecht, doi:10.1007/978-94-017-8598-3, 2014.

de Groot, W. J., Flannigan, M. D., and Cantin, A. S.: Climate change impacts on future boreal fire regimes, Forest Ecol. Manage., 294, 35–44, doi:10.1016/j.foreco.2012.09.027, 2013b.

de Groot, W. J., Goldammer, J. G., Keenan, T., Brady, M. A., Lynham, T. J., Justice, C. O., Csiszar, I. A., and Loughlin, K. O.: Developing a global early warning system for wildland fire, in: V International Conference on Forest Fire Research, edited by: Viegas, D., p. 12, Coimbra, Portugal, 2006.

Diez, E. L. G., Salazar, J. L. L., and Davila, F. D.: Some meteorological conditions associated with forest-fires in Galicia (Spain), Int. J. Biometeorol., 37, 194–199, 1993.

Dowdy, A. J., Mills, G. A., Finkele, K., and de Groot, W.: Index sensitivity analysis applied to the Canadian Forest Fire Weather Index and the McArthur Forest Fire Danger Index, Meteorol. Appl., 17, 298–312, doi:10.1002/met.170, 2010.

Dowdy, A. J., Mills, G. A., Finkele, K., and de Groot, W. J.: Australian fire weather as represented by the McArthur Forest Fire Danger Index and the Canadian Forest Fire Weather Index Rep., 84 pp., Centre for Australian Weather and Climate Research, 2009.

Entekhabi, D., Njoku, E. G., O'Neill, P. E., Kellogg, K. H., Crow, W. T., Edelstein, W. N., Entin, J. K., Goodman, S. D., Jackson, T. J., Johnson, J., Kimball, J., Piepmeier, J. R., Koster, R. D., Martin, N., McDonald, K. C., Moghaddam, M., Moran, S., Reichle, R., Shi, J.-C., Spencer, M. W., Thurman, S. W., Leung Tsang, and Van Zyl, J. : The Soil Moisture Active Passive (SMAP) Mission, Proc. IEEE, 98, 704–716, doi:10.1109/jproc.2010.2043918, 2010.

Fernandes, K., Baethgen, W., Bernardes, S., DeFries, R., DeWitt, D. G., Goddard, L., Lavado, W., Lee, D. E., Padoch, C., Pinedo-Vasquez, M., and Uriarte, M.: North Tropical Atlantic influence on western Amazon fire season variability, Geophys. Res. Lett., 38, L12701, doi:10.1029/2011GL047392, 2011.

Field, R. D. and Shen, S. S. P.: Predictability of carbon emissions from biomass burning in Indonesia from 1997 to 2006, J. Geophys. Res., 113, G04024, doi:10.1029/2008JG000694, 2008.

Field, R. D., Wang, Y., Roswintiarti, O., and Guswanto: A drought-based predictor of recent haze events in western Indonesia, Atmos. Environ., 38, 1869–1878, doi:10.1016/j.atmosenv.2004.01.011, 2004.

Field, R. D., van der Werf, G. R., and Shen, S. S. P.: Human amplification of drought-induced biomass burning in Indonesia since 1960, Nat. Geosci., 2, 185–188, doi:10.1038/ngeo443, 2009.

Flannigan, M., Cantin, A. S., de Groot, W. J., Wotton, M., Newbery, A., and Gowman, L. M.: Global wildland fire season severity in the 21st century, Forest Ecol. Manage., 294, 54–61, doi:10.1016/j.foreco.2012.10.022, 2013.

Forsyth, T.: Public concerns about transboundary haze: A comparison of Indonesia, Singapore, and Malaysia, Global Environ. Change-Human Pol. Dimensions, 25, 76–86, doi:10.1016/j.gloenvcha.2014.01.013, 2014.

Giglio, L., Randerson, J. T., and van der Werf, G. R.: Analysis of daily, monthly, and annual burned area using the fourth-generation global fire emissions database (GFED4), J. Geophys. Res.-Biogeosci., 118, 317–328, doi:10.1002/jgrg.20042, 2013.

Haines, D. A.: A lower atmospheric severity index for wildland fires, National Weather Digest, 13, 23–27, 1988.

Hincks, T. K., Malamud, B. D., Sparks, R. S. J., Wooster, M. J., and Lynham, T. J.: Risk assessment and management of wildfires, in: Risk and Uncertainty Assessment for Natural Hazards, edited by: Rougier, J., Sparks, S. and Hill, L., 398–444, Cambridge University Press, Cambridge, UK, doi:10.1017/CBO9781139047562.013, 2013.

Horel, J., Ziel, R., Galli, C., Pechmann, J., and Dong, X.: An evaluation of Fire Danger and Behaviour Indices in the Great Lakes Region Calculated from Station and Gridded Weather Information, Int. J. Wildland Fire, 23, 202–214, doi:10.1071/WF12186, 2014.

Hoscilo, A., Page, S. E., Tansey, K. J., and Rieley, J. O.: Effect of repeated fires on land-cover change on peatland in southern Central Kalimantan, Indonesia, from 1973 to 2005, Int. J. Wildland Fire, 20, 578–588, doi:10.1071/wf10029, 2011.

Huffman, G. J., Adler, R. F., Bolvin, D. T., and Gu, G.: Improving the global precipitation record: GPCP Version 2.1, Geophys. Res. Lett., 36, L17808, doi:10.1029/2009gl040000, 2009.

Huffman, G. J., Adler, R. F., Bolvin, D. T., Gu, G., Nelkin, E. J., Bowman, K. P., Hong, Y., Stocker, E. F., and Wolff, D. B.: The TRMM multisatellite precipitation analysis (TMPA): Quasi-global, multiyear, combined-sensor precipitation estimates at fine scales, J. Hydrometeorol., 8, 38–55, doi:10.1175/jhm560.1, 2007.

Jiang, Y., Zhuang, Q., Flannigan, M. D., and Little, J. M.: Characterization of wildfire regimes in Canadian boreal terrestrial ecosystems, Int. J. Wildland Fire, 18, 992–1002, doi:10.1071/wf08096, 2009.

Kalnay, E., Kanamitsu, M., Kistler, R., et al.: The NCEP/NCAR 40-year reanalysis project, B. Am. Meteorol. Soc., 77, 437–471, doi:10.1175/1520-0477(1996)077<0437:tnyrp> 2.0.co;2, 1996.

Keeley, J. E., Bond, W. J., Bradstock, R. A., Pausas, J. G., and Rundel, P. W.: Fire in Mediterranean Ecosystems: Ecology, Evolution and Management, 522 pp., Cambridge University Press, Cambridge, 2011.

Kerr, Y. H., Waldteufel, P., Wigneron, J.-P., Delwart, S., Cabot, F., Boutin, J., Escorihuela, M.-J., Font, J., Reul, N., Gruhier, C., Juglea, S. E., Drinkwater, M. R., Hahne, A., Martin-Neira, M., and Mecklenburg, S.: The SMOS Mission: New Tool for Monitoring Key Elements of the Global Water Cycle, Proc. IEEE, 98, 666–687, doi:10.1109/jproc.2010.2043032, 2010.

Langner, A. and Siegert, F.: Spatiotemporal fire occurrence in Borneo over a period of 10 years, Global Change Biol., 15, 48–62, doi:10.1111/j.1365-2486.2008.01828.x, 2009.

Lawson, B. D. and Armitage, O. B.: Weather guide for the Canadian Forest Fire Danger Rating SystemRep., 73 pp., Northern Forestry Centre, Edmonton, Canada, 2008.

Lee, B. S., Alexander, M. E., Hawkes, B. C., Lynham, T. J., Stocks, B. J., and Englefield, P.: Information systems in support of wildland fire management decision making in Canada, Comput. Electron. Agr., 37, 185–198, doi:10.1016/s0168-1699(02)00120-5, 2002.

Lehsten, V., de Groot, W. J., Flannigan, M., George, C., Harmand, P., and Balzter, H.: Wildfires in boreal ecoregions: Evaluating the power law assumption and intra-annual and inter-annual variations, J. Geophys. Res.-Biogeosci., 119, 14–23, doi:10.1002/2012jg002252, 2014.

Lorenz, C. and Kunstmann, H.: The Hydrological Cycle in Three State-of-the-Art Reanalyses: Intercomparison and Performance Analysis, J. Hydrometeorol., 13, 1397–1420, doi:10.1175/jhm-d-11-088.1, 2012.

Lucas, C.: On developing a historical fire weather data-set for Australia, Aust. Meteorol. Oceanogr. J., 60, 1–13, 2010.

Luke, R. H. and McArthur, A. G.: Bushfires in Australia, 359 pp., Australia Forestry and Timber Bureau, Commonwealth Scientific and Industrial Research Organization, Division of Forest Research, Canberra, 1978.

Manomaiphiboon, K., Octaviani, M., Torsri, K., and Towprayoon, S.: Projected changes in means and extremes of temperature and precipitation over Thailand under three future emissions scenarios, Clim. Res., 58, 97–115, doi:10.3354/cr01188, 2013.

McArthur, A. G.: Fire behaviour in Eucalyptus Forests Rep., Department of National Development Forestry and Timber Bureau, Canberra, 1967.

Merrill, D. F. and Alexander, M. E.: Glossary of Forest Fire Management Terms Rep., National Research Council of Canada, Ottawa, Ontario, Canada, 1987.

Millington, J. D. A., Perry, G. L. W., and Malamud, B. D.: Models, data and mechanisms: quantifying wildfire regimes, in: Fractal Analysis for Natural Hazards, edited by: Cello, G. and Malamud, B. D., 155–167, Geological Society of London, Special Publications, London, UK, 2006.

Minnich, R. A. and Chou, Y. H.: Wildland fire patch dynamics in the chaparral of southern California and northern Baja California, Int. J. Wildland Fire, 7, 221–248, doi:10.1071/wf9970221, 1997.

Mitchell, T. D. and Jones, P. D.: An improved method of constructing a database of monthly climate observations and associated high-resolution grids, Int. J. Climatol., 25, 693–712, doi:10.1002/joc.1181, 2005.

Monzon-Alvarado, C., Cortina-Villar, S., Schmook, B., Flamenco-Sandoval, A., Christman, Z., and Arriola, L.: Land-use decision-making after large-scale forest fires: Analyzing fires as a driver of deforestation in Laguna del Tigre National Park, Guatemala, Appl. Geogr., 35, 43–52, doi:10.1016/j.apgeog.2012.04.008, 2012.

Morton, D. C., Le Page, Y., DeFries, R., Collatz, G. J., and Hurtt, G. C.: Understorey fire frequency and the fate of burned forests in southern Amazonia, Philos. Trans. Roy. Soc. B, 368, 20120163, doi:10.1098/rstb.2012.0163, 2013.

Mukherjee, I. and Sovacool, B. K.: Palm oil-based biofuels and sustainability in southeast Asia: A review of Indonesia, Malaysia and Thailand, Renew. Sustain. Energy Rev., 37, 1–12, 2014.

Nguyen, T. K. O. and Leelasakultum, K.: Analysis of meteorology and emission in haze episode prevalence over mountain-bounded region for early warning, Sci. Total Environ., 409, 2261–2271, doi:10.1016/j.scitotenv.2011.02.022, 2011.

Noble, I. R., Barry, G. A. V., and Gill, A. M.: McArthur's Fire-Danger Meters Expressed as Equations, Aust. J. Ecol., 5, 201–203, 1980.

Paciorek, C. J., Risbey, J. S., Ventura, V., and Rosen, R. D.: Multiple indices of Northern Hemisphere cyclone activity, winters 1949–99, J. Climate, 15, 1573–1590, doi:10.1175/1520-0442(2002)015<1573:mionhc>2.0.co;2, 2002.

Padilla, M. and Vega-Garcia, C.: On the comparative importance of fire danger rating indices and their integration with spatial and temporal variables for predicting daily human-caused fire occurrences in Spain, Int. J. Wildland Fire, 20, 46–58, doi:10.1071/wf09139, 2011.

Pausas, J. G. and Paula, S.: Fuel shapes the fire-climate relationship: evidence from Mediterranean ecosystems, Global Ecol. Biogeogr., 21, 1074–1082, doi:10.1111/j.1466-8238.2012.00769.x, 2012.

Pellizzaro, G., Cesaraccio, C., Duce, P., Ventura, A., and Zara, P.: Relationships between seasonal patterns of live fuel moisture and meteorological drought indices for Mediterranean shrubland species, Int. J. Wildland Fire, 16, 232–241, doi:10.1071/wf06081, 2007.

Reynolds, R. W., Rayner, N. A., Smith, T. M., Stokes, D. C., and Wang, W. Q.: An improved in situ and satellite SST analysis for climate, J. Climate, 15, 1609–1625, doi:10.1175/1520-0442(2002)015<1609:aiisas> 2.0.co;2, 2002.

Rienecker, M. M., Suarez, M. J., Gelaro, R., et al.: MERRA: NASA's Modern-Era Retrospective Analysis for Research and Applications, J. Climate, 24, 3624–3648, doi:10.1175/jcli-d-11-00015.1, 2011.

Russell-Smith, J., Yates, C. P., Whitehead, P. J., Smith, R., Craig, R., Allan, G. E., Thackway, R., Frakes, I., Cridland, S., Meyer, M. C. P., and Gill A. M.: Bushfires ′down under′: patterns and implications of contemporary Australian landscape burning, Int. J. Wildland Fire, 16, 361–377, doi:10.1071/wf07018, 2007.

Sheffield, J., Goteti, G., and Wood, E. F.: Development of a 50-year high-resolution global dataset of meteorological forcings for land surface modeling, J. Climate, 19, 3088–3111, doi:10.1175/jcli3790.1, 2006.

Smith, A., Lott, N., and Vose, R.: The Integrated Surface Database Recent Developments and Partnerships, B. Am. Meteorol. Soc., 92, 704–708, doi:10.1175/2011bams3015.1, 2011.

Smith, E. A., Asrar, G., Furuhama, Y., et al.: International Global Precipitation Measurement (GPM) Program and Mission: An Overview, Measuring Precipitation from Space: Eurainsat and the Future, 28, 611–653, doi:10.1007/978-1-4020-5835-6_48, 2007.

Spessa, A. C., Field, R. D., Pappenberger, F., Langner, A., Englhart, S., Weber, U., Stockdale, T., Siegert, F., Kaiser, J. W., and Moore, J.: Seasonal forecasting of fire over Kalimantan, Indonesia, Nat. Hazards Earth Syst. Sci., 15, 429–442, doi:10.5194/nhess-15-429-2015, 2015.

Stocks, B. J., Mason, J. A., Todd, J. B., Bosch, E. M., Wotton, B. M., Amiro, B. D., Flannigan, M. D., Hirsch, K. G., Logan, K. A., Martell, D. L., and Skinner, W. R.: Large forest fires in Canada, 1959–1997, J. Geophys. Res., 108, 8149, doi:10.1029/2001jd000484, 2002.

Tanpipat, V., Honda, K., and Nuchaiya, P.: MODIS Hotspot Validation over Thailand, Remote Sens., 1, 1043–1054, doi:10.3390/rs1041043, 2009.

Taylor, S. W. and Alexander, M. E.: Science, technology, and human factors in fire danger rating: the Canadian experience, Int. J. Wildland Fire, 15, 121–135, doi:10.1071/wf05021, 2006.

Thonicke, K., Spessa, A., Prentice, I. C., Harrison, S. P., Dong, L., and Carmona-Moreno, C.: The influence of vegetation, fire spread and fire behaviour on biomass burning and trace gas emissions: results from a process-based model, Biogeosciences, 7, 1991–2011, doi:10.5194/bg-7-1991-2010, 2010.

van der Werf, G. R., Dempewolf, J., Trigg, S. N., Randerson, J. T., Kasibhatla, P. S., Giglio, L., Murdiyarso, D., Peters, W., Morton, D. C., Collatz, G. J., Dolman, A. J., and DeFries, R. S.: Climate regulation of fire emissions and deforestation in equatorial Asia, P. Natl. Acad. Sci. USA, 105, 20350–20355, doi:10.1073/pnas.0803375105, 2008.

van der Werf, G. R., Randerson, J. T., Giglio, L., Collatz, G. J., Mu, M., Kasibhatla, P. S., Morton, D. C., DeFries, R. S., Jin, Y., and van Leeuwen, T. T.: Global fire emissions and the contribution of deforestation, savanna, forest, agricultural, and peat fires (1997–2009), Atmos. Chem. Phys., 10, 11707–11735, doi:10.5194/acp-10-11707-2010, 2010.

Van Wagner, C. E.: Development and structure of the Canadian Forest Fire Weather Index SystemRep., 37 pp., Canadian Forest Service, Ottawa, Canada, 1987.

Veblen, T. T.: Forest preservation in western highlands of Guatemala, Geogr. Rev., 68, 417-434, doi:10.2307/214215, 1978.

Wastl, C., Schunk, C., Luepke, M., Cocca, G., Conedera, M., Valese, E., and Menzel, A.: Large-scale weather types, forest fire danger, and wildfire occurrence in the Alps, Agr. Forest Meteorol., 168, 15–25, doi:10.1016/j.agrformet.2012.08.011, 2013.

Wotton, B. M. and Flannigan, M. D.: Length of the fire season in a changing climate, Forest. Chronicle, 69, 187–192, 1993.

Zumbrunnen, T., Bugmann, H., Conedera, M., and Buergi, M.: Linking Forest Fire Regimes and Climate-A Historical Analysis in a Dry Inner Alpine Valley, Ecosystems, 12, 73–86, doi:10.1007/s10021-008-9207-3, 2009.